Original article

Investigating metal-organic framework as a new *pseudo*-capacitive material for supercapacitors

Long Kang [a], Shi-Xiong Sun [a], Ling-Bin Kong [a,*], Jun-Wei Lang [b], Yong-Chun Luo [a]

[a] *State Key Laboratory of Advanced Processing and Recycling of Non-ferrous Metals, Lanzhou University of Technology, Lanzhou 730050, China*
[b] *Laboratory of Clean Energy Chemistry and Materials, Lanzhou Institute of Chemical Physics, Chinese Academy of Science, Lanzhou 730000, China*

A B S T R A C T

A new application of metal organic framework (MOF) as a *pseudo*-capacitive material for supercapacitors is investigated. To this end, a simple nickel-based MOF, formulated $Ni_3(btc)_2 \cdot 12H_2O$, is synthesized *via* a hydrothermal reaction. As an electro-active material, such nickel-based MOF exhibits superior *pseudo*-capacitive behavior in KOH aqueous electrolyte with a high specific capacitance of 726 F g^{-1}. Also, it displays good electrochemical stability with 94.6% of the initial capacitance over consecutive 1000 cycles. In addition, a simple asymmetric supercapacitor with a high energy density of 16.5 Wh kg^{-1} is successfully built using the nickel-based MOF as positive electrode and commercial activated carbon as negative electrode in KOH electrolyte.

© 2014 Ling-Bin Kong. Published by Elsevier B.V. on behalf of Chinese Chemical Society. All rights reserved.

1. Introduction

Supercapacitors, as energy storage and conversion devices with high power density and fast recharge capability, have promising applications as backup or auxiliary power sources in electric vehicles and other electronic devices [1,2]. On the basis of the charge storage mechanisms, supercapacitors can be classified into two types: One is the electrical double-layer capacitors (EDLCs), where the capacitance arises from the charge separation at an electrode/electrolyte interface; the other is the *pseudo*-capacitor, where the capacitance arises from the fast and reversible redox reactions at the surfaces of the electroactive materials [3–6].

Up to now, various carbon materials, such as activated carbon [7], carbon fibers [8], carbon aerogels [9], carbon nanotubes [10], and grapheme [11], have been used as the electrode materials for EDLCs. Also, some metal oxides/hydroxides (RuO_2 [12], MnO_2 [13], Co_3O_4 [14], NiO [15], $Co(OH)_2$ [16], $Ni(OH)_2$ [17], *etc.*) and conducting polymers (polyaniline [18] and polypyrrole [19]) have been extensively studied as electro-active materials for *pseudo*-capacitors.

Metal organic frameworks (MOFs), a class of crystalline and highly porous hybrid materials obtained by the assembly of metallic ions and organic ligands, have attracted intense interest owing to their wide potential applications in catalysis, magnetism, luminescence, sensors, drug delivery, and particularly in gas storage and separation. These properties and utilities of MOFs depend on their pore size and shape, the interior and exterior surfaces, and the functional groups [20–22].

More recently, MOFs have been successfully used as electrode materials for rechargeable batteries and fuel cells because the redox behavior of metal cations inside MOFs provides a pathway for electrons, and the linker structure promotes charge transfer inside the framework [23,24]. The introduction of MOFs in supercapacitors has been reported only recently. Díaz *et al.* reported for the first time the electrical double-layer capacitive behavior of a Zn-based MOF partially substituted with Co; a gravimetric capacitance of only 2 F g^{-1} was estimated [25]. Lee *et al.* synthesized a Co-based MOF and investigated its capacitive behavior in various aqueous electrolytes. The result of the study showed that the Co-based MOF show an interesting *pseudo*-capacitive behavior in LiOH electrolyte [26]. Thus, Morozan *et al.* deduced that MOFs with abundant porous structure, high surface areas, and incorporated *pseudo*-capacitive redox centers would be possible candidates as electrode materials for supercapacitors [27]. However, no more convincing experimental instances have been reported to identify such a MOF.

In this work, Ni(II) chloride hydrate and H_3btc has been employed for the first time to synthesize Ni-based MOFs materials. The hydrothermal reaction of Ni(II) nitrate hydrate with H_3btc acid yields green crystals formulated as $Ni_3(btc)_2 \cdot 12H_2O$ with a

* Corresponding author.
E-mail address: konglb@lut.cn (L.-B. Kong).

structure composed of zigzag chains with both the bridging and terminal Ni^{2+} ions and each nickel center coordinated to four water molecules. The electrochemical properties of the prepared Ni-based MOF are explored. The test results show that the nickel-based MOF exhibits superior *pseudo*-capacitive behavior in KOH aqueous electrolyte with a high specific capacitance of 726 F g^{-1} and good cyclical stability.

2. Experimental

2.1. Synthesis of nickel-based MOF

All solvents and reagents for the syntheses were of analytical grade and were used as received from commercial sources without further purification. A mixture of Ni(Cl)$_2$·6H$_2$O (3.0 mmol), H$_3$btc (1.0 mmol), DMF (N,N-dimethylformamide) (5.0 mL) and distilled water (5.0 mL) was placed in a 25 mL Teflon-lined stainless autoclave. The autoclave was sealed, heated to 105 °C, kept at 105 °C under autogenous pressure for 2 days, and then cooled to room temperature. The as-obtained green crystals were filtered, washed with DMF and distilled water, and then air-dried to give about 0.29 g of Ni-based MOF (yield of 71% based on H$_3$btc). Anal. Calcd. for C$_{18}$H$_{30}$Ni$_3$O$_{24}$ (Mr = 806.5): C 26.81, H 3.75; found: C 26.43, H 3.54.

2.2. Stuctural characterization

A single crystal was selected and attached to a glass fiber using epoxy. Crystal data were collected on a Bruker SMART APEX II diffractometer at room temperature with graphite-monochromated Mo Kα radiation (λ = 0.71073 Å). The structures were analyzed by direct methods using the SHELXS program.

2.3. Electrochemical measurements in three-electrode system and two electrode system

The electrochemical measurements were carried out using an electrochemical working station (CHI660D, Shanghai, China) in 2 mol L^{-1} KOH electrolyte at room temperature. The cyclic voltammetry (CV) measurements were conducted at different scan rates ranging from 2.5 mV s^{-1} to 20 mV s^{-1}. Electrochemical impedance spectroscopy (EIS) measurements were recorded from 10 kHz to 0.1 Hz with an alternate current amplitude of 5 mV. Galvanostatic charge/discharge measurements were run at different current densities ranging from 0.25 A g^{-1} to 5 A g^{-1}.

For the three-electrode system, the working electrode contained about 8 mg of electroactive material. A platinum gauze electrode and a saturated calomel electrode (SCE) served as the counter electrode and the reference electrode, respectively. The corresponding specific capacitance was calculated from:

$$C \ (\text{F g}^{-1}) = \frac{I}{(dE/dt) \times m} \approx \frac{I}{(\Delta E/\Delta t) \times m} \qquad (1)$$

where C is the specific capacitance, I is the constant discharging current, dE/dt indicates the slope of the discharging curves, and m is the mass of the corresponding electrode material.

For two-electrode system, the Ni-based MOF cathode and commercial capacitive activated carbon (AC, purchased from Kuraray Co., Ltd., Japan) anode electrode were pressed together and separated by a porous nonwoven cloth separator. The electrode contained about 4 mg and 8 mg (according to the equation: C' = IΔt/m, the charge on the MOF and AC electrode are 291 and 152 C g^{-1}, respectively. Therefore, the optimal mass ratio of the MOF and AC electrodes in the asymmetric supercapacitor cell is 152:291) of electroactive material for the cathode and anode electrode, respectively. Moreover, a symmetric EDLC (AC/AC) was

fabricated for comparison, and each AC electrode contained about 6 mg of electroactive material.

The specific capacitance of the supercapacitor cell can be evaluated from the charge/discharge test together with the following equation:

$$C_\text{T} \ (\text{F g}^{-1}) = \frac{I\Delta t}{\Delta E} \times m \qquad (2)$$

where I in A is the constant discharging current; Δt in s is the discharge time; ΔE in V is the potential window during the discharge process after IR drop; and m in g is the total mass of the two electrode materials.

The specific energy density and power density are defined as

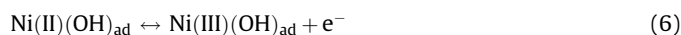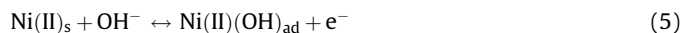$$E \ (\text{Wh kg}^{-1}) = \frac{0.5 C_\text{T} V^2}{3.6} \qquad (3)$$

$$P \ (\text{kW kg}^{-1}) = \frac{E \times 3600}{t} \qquad (4)$$

where V in V is the voltage change during the discharge process after IR drop, and t in s is the discharge time.

3. Results and discussion

A complete single crystal analysis was undertaken on the as-prepared Ni-based MOF, and the crystallographic details of the Ni-based MOF were found to have identical cell parameters and single-crystal structure to that of a previously reported cobalt-based MOF [28]. The structural representation of the Ni-based MOF compound is shown in Fig. 1. As shown in Fig. 1(a), the structure of the as-prepared compound is composed of 1-dimentional (1D) zigzag chains constructed from two symmetry-inequivalent tetra-aqua nickel (II) units and BTC ligands. As shown in Fig. 1(b), these 1D chains can be reinforced and crosslinked into a complicated 3D network by extensive hydrogen bonding interactions, where every water proton is involved in a hydrogen bond to either a carboxylate or water oxygen.

The electrochemical properties of the as-made MOF were investigated under a three-electrode system in KOH aqueous electrolyte. Fig. 2(a) shows the cyclic voltammetry (CV) curves of the Ni-based MOF electrode at different sweep rates. The shape of the CV curves reveals that the capacitance characteristic is well distinguished from that of the EDLCs in which the shape is normally close to an ideal rectangular shape [29]. A couple of redox peaks are observed within the potential range from 0 to 0.5 V. Two plausible reactions may occur as *quasi*-reversible redox processes during the potential sweep:

$$\text{Ni(II)}_\text{s} + \text{OH}^- \leftrightarrow \text{Ni(II)(OH)}_\text{ad} + \text{e}^- \qquad (5)$$

$$\text{Ni(II)(OH)}_\text{ad} \leftrightarrow \text{Ni(III)(OH)}_\text{ad} + \text{e}^- \qquad (6)$$

The anodic peak is due to the oxidation of Ni(II) to Ni(III) and the cathodic peak is for the reverse process [30]. It indicates that the capacitance mainly results from the *pseudo*-capacitive capacitance, which is based on a redox mechanism. It should be noted that with the sweep rate increases, the increment in the area of the CV and its current response is observed. This indicates that the nickel-based MOF is favorable for fast reversible faradaic reactions.

Fig. 2(b) shows the galvanostatic charge/discharge curves of the Ni-based MOF electrode within a potential window of 0–0.4 V at different current densities. The shape of the discharge curves does not display the characteristics of a pure EDLC, but mainly *pseudo*-capacitance, which is in agreement with the result from the CV curves. The corresponding specific capacitance of the MOF electrode at 1 A g^{-1} was calculated to be 726 F g^{-1}. As the discharge current density increases from 1 A g^{-1} to 5 A g^{-1}, a large voltage drop is observed, and finally the capacitance decreases from 726 F g^{-1} to